frontiers | Frontiers in Chemistry

TYPE Original Research
PUBLISHED 17 January 2023
DOI 10.3389/fchem.2022.1096014

OPEN ACCESS

EDITED BY
Simón Poblete,
Universidad Austral de Chile, Chile

REVIEWED BY
Marco Zoli,
University of Camerino, Italy
Antonio Suma,
University of Bari Aldo Moro, Italy

*CORRESPONDENCE
Peter Virnau,
virnau@uni-mainz.de

SPECIALTY SECTION
This article was submitted to Theoretical and Computational Chemistry, a section of the journal Frontiers in Chemistry

RECEIVED 11 November 2022
ACCEPTED 23 December 2022
PUBLISHED 17 January 2023

CITATION
Wettermann S, Datta R and Virnau P (2023), Influence of ionic conditions on knotting in a coarse-grained model for DNA. *Front. Chem.* 10:1096014. doi: 10.3389/fchem.2022.1096014

Influence of ionic conditions on knotting in a coarse-grained model for DNA

Sarah Wettermann, Ranajay Datta and Peter Virnau*

Institut für Physik, Johannes Gutenberg-Universität, Mainz, Germany

We investigate knotting probabilities of long double-stranded DNA strands in a coarse-grained Kratky-Porod model for DNA with Monte Carlo simulations. Various ionic conditions are implemented by adjusting the effective diameter of monomers. We find that the occurrence of knots in DNA can be reinforced considerably by high salt conditions and confinement between plates. Likewise, knots can almost be dissolved completely in a low salt scenario. Comparisons with recent experiments confirm that the coarse-grained model is able to capture and quantitatively predict topological features of DNA and can be used for guiding future experiments on DNA knots.

KEYWORDS

polymers, ionic conditions, knots, coarse-grained model, DNA

Introduction

The revelation of DNA packing and folding in the cell nucleus (Lieberman-Aiden et al., 2009; Siebert et al., 2017; Stevens et al., 2017; Ganji et al., 2018) and the emergence of commercially available nanopore techniques (Jain et al., 2016; Jain et al., 2018) has ushered in a new era of DNA research in the past decade. Knots, which emerge naturally as a byproduct in long macromolecules like DNA (Frisch and Wasserman, 1961; Delbrück, 1962), may however be detrimental to biological processes and technical applications. It is therefore of prime importance to study conditions and length scales at which they appear in equilibrium and develop strategies to enhance (Lua et al., 2004; Virnau et al., 2005; Tang et al., 2011; Amin et al., 2018) or suppress knotting (Di Stefano et al., 2014; Renner and Doyle, 2014). From a technical point of view, numerical simulations are a great tool for this task as structural and topological information are readily available. Coarse-grained models are particularly relevant as knots appear at scales beyond the Kuhn length and models with atomistic resolution are often poorly suited for efficient Monte Carlo algorithms required to scan configuration space. It is therefore crucial to test and improve coarse-grained models for DNA to quantitatively support and interpret experimental efforts.

A first link to double-stranded (ds) DNA was already established in the first simulation paper on polymer knots from 1974 (Vologodskii et al., 1974). In their seminal contribution, Vologodskii et al. determined knotting probabilities of random walks and associated single segments with the Kuhn length of DNA (100 *nm*)—a prediction which turns out to be surprisingly accurate as we will demonstrate later. This basic approach has been refined further in the early 1990s in conjunction with gel electrophoresis experiments on short DNA strands of up to 10 kbp (Rybenkov et al., 1993; Shaw and Wang, 1994). Ideal segments were replaced by cylinders with excluded volume interactions that depend on ionic conditions (Rybenkov et al., 1993), and it was also demonstrated that DNA knotting probabilities vary somewhat with solvent conditions (reaching about 4% in a high salt environment.) Higher resolution versions of this model in which one Kuhn length is represented by several segments have been used to study the effect of confinement on short strands in high salt conditions. Among other things, Orlandini, Micheletti and coworkers have

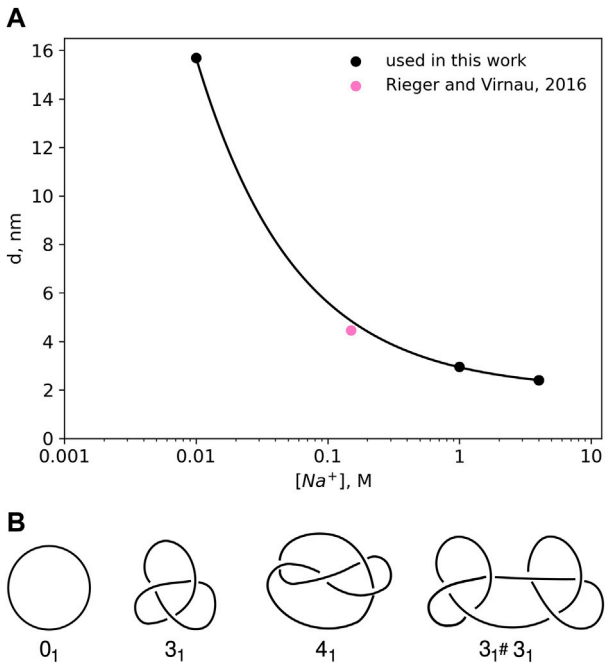

FIGURE 1
(A) Effective diameter of DNA, *d* as a function of NaCl concentration as calculated by Stigter (1977) on the basis of polyelectrolyte theory. The values for the effective diameter, *d* have been obtained by calculating the interaction potentials of highly charged colloidal cylinders representing DNA. The effective diameter value for physiological salt concentrations 0.15 M has been taken from Rieger and Virnau (2016). **(B)** Knot types considered in this paper.

demonstrated with numerical simulations that confining DNA between plates or in nanopores increases knotting probabilities when typical distances between plates or nanopore diameters are in the order of the Kuhn length of DNA (Micheletti and Orlandini, 2012a; Micheletti and Orlandini, 2012b; Orlandini and Micheletti, 2013). Alternatively, coarse-grained bead-stick (Dai et al., 2012a; Dai et al., 2012b; Rieger and Virnau, 2016) or bead-spring (Trefz et al., 2014; Rothörl et al., 2022) representations for DNA can be used in which the effective diameter is adjusted to account for varying solvent conditions and which can be adapted for molecular dynamics simulations. Of particular relevance to our study is Dai et al. (2012b) in which the authors have studied knotting of closed DNA rings in bulk and plate geometry and to which our results for open strands can be compared. Variants of this model class have also been applied to investigate, e.g., statics (Dai et al., 2015; Jain and Dorfman, 2017) and dynamics of DNA knots in a nanochannel (Micheletti and Orlandini, 2014), packing of DNA in viral capsids (Marenduzzo et al., 2009; Reith et al., 2012) and recently for the reproduction of experimental knotting probabilities of λ phage DNA in high salt conditions (Kumar Sharma et al., 2019). Of course, there are also limits to this class of coarse-grained descriptions, and higher resolution models (Suma and Micheletti, 2017; Suma et al., 2018) may address questions which either require a detailed structural description or an explicit modelling of electrostatic interactions (Suma et al., 2018).

In this work we systematically extend previous analyses to DNA lengths relevant to modern experiments on λ (Plesa et al., 2016; Kumar Sharma et al., 2019) and *T*4 phages (Plesa et al., 2016). Our comprehensive study also covers the full range of ionic conditions for free DNA and DNA confined between two plates, and comparisons with existing experimental data confirm the validity of the modelling approach. This enables us to show, amongst others, that for the considered strand sizes the dependence of knotting on salt concentrations (Rybenkov et al., 1993) can be used to effectively disentangle DNA prior to experiments where knots are undesired.

Methods

Implicit modelling of ionic solvent conditions

DNA is negatively charged, but long-range electrostatic interactions are partially or completely screened by counterions in solution. In this paper we follow an implicit solvent approach pioneered by Stigter (1977) and Rybenkov et al. (1993) in which screened charges are represented by effective excluded volume interactions. The diameter *d* of a DNA chain is a parameter that quantifies the latter and can be defined as the segment diameter of a representative chain which is uncharged, but has the same configurational and morphological properties as the original DNA with partial or completely screened charges. The magnitude of the electrostatic repulsion, and consequently, the numerical value of *d*, is a function of salt concentration. Stigter (1977) modeled DNA in sodium chloride solution as charged cylinders. Following the theory developed by McMillan and Mayer (1945) and the calculations of Hill (Hill, 1956; Hill, 1960), Stigter carried out analytic calculations to estimate the effective diameter of DNA as a function of sodium chloride concentration (see Figure 1A).

Already in 1993 Rybenkov et al. (1993) were able to confirm this approach (and Figure 1A) by representing DNA as a closed chain of cylinders of Kuhn length 100 nm and by matching experimentally determined knotting probabilities of a short *P*4 phage DNA strand (of around 10,000 base pairs) with those obtained from Monte Carlo simulations.

Here, we use a higher resolution variation of this ansatz which models DNA as a standard bead-stick chain and also resolves local structure at the scale of the persistence length (which according to Kratky-Porod theory is half of the Kuhn length). We keep, however, the same effective diameter to determine knotting probabilities in various ionic conditions for long, experimentally relevant DNA strands (like λ phage or T4). In a previous work (Rieger and Virnau, 2016), we have already validated this approach by determining simulation parameters for physiological conditions ($0.15M$) that reproduce experimental knotting spectra of short strands from Rybenkov et al. (1993) and Shaw and Wang (1994) even without making assumptions about the persistence or Kuhn length. Not only did these simulations confirm a value for *d* which is close to the value of Stigter (pink point in Figure 1A), they also confirmed the correct persistence length of DNA. While we use $d = 4.465$ nm for physiological conditions, values for other ionic conditions are directly taken from Figure 1A.

Bead-stick model. Simulations were performed using a discrete Kratky-Porod model (Kratky and Porod, 1949; Dai et al., 2012b; Marenz and Janke, 2016; Rieger and Virnau, 2016) with hard sphere interactions between monomers and a constant distance between adjacent beads. For simulations in slit confinement, walls are also hard and impenetrable. Chain stiffness is implemented *via* a bond-bending potential:

$$U = \kappa \sum_i (1 - \cos\theta_i) \tag{1}$$

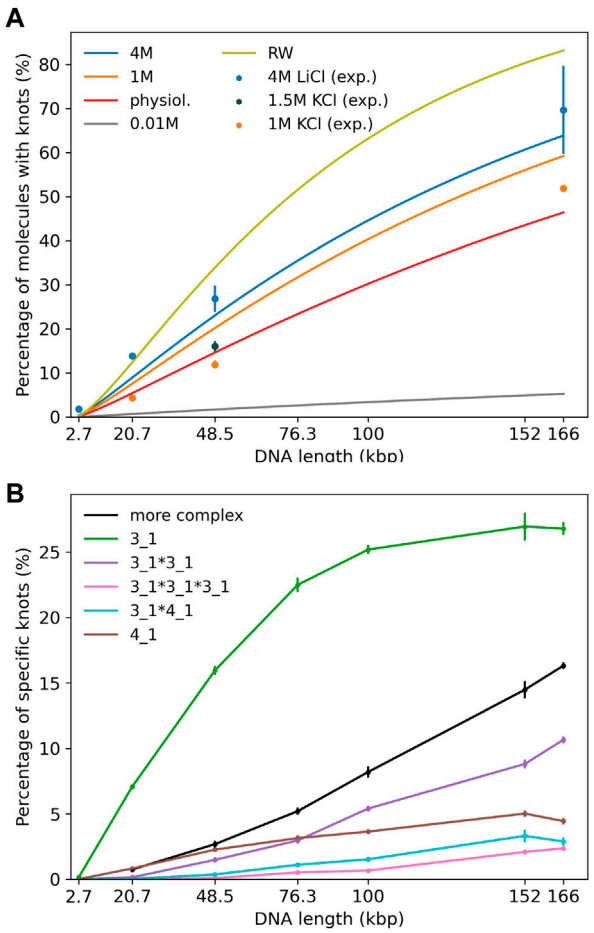

FIGURE 2
(A) Knotting probability as a function of chain length for DNA chains of up to 166 kbp in comparison to recent experiments (Plesa et al., 2016; Kumar Sharma et al., 2019). Straight lines refer to simulations and data points to experiments. Different colors represent varying ionic conditions. **(B)** Knot spectrum as a function of DNA length for simulations in a high salt solvent (4 M) scenario. Complex knots refer to all other knots not listed here excluding the unknot.

where θ_i for $i = 1, \ldots, N-1$ are the angles between adjacent bond vectors. Simulations were performed at various salt concentrations with values for d obtained from Figure 1A. We assume a persistence length l_p of 50 nm or 150 base pairs (bp) for all considered salt concentrations. For a Kratky-Porod chain the stiffness parameter κ for any given effective diameter d can be computed as (Fisher, 1964; Trefz et al., 2014; Rieger and Virnau, 2016)

$$\kappa \approx \frac{l_p \cdot k_B T}{d}. \tag{2}$$

In dsDNA the distance between adjacent base pairs is 1/3 nm. By comparing the contour lengths, we conclude that a DNA strand with B base pairs is represented by a chain of

$$N \approx B \cdot 0.3333 \text{ nm}/d \tag{3}$$

beads.

Several simplifications are implied in this approach. The dependence of persistence length on ionic conditions was neglected as differences only amount to a few percent at least in the formalism of Odijk (1977); Skolnick and Fixman (1977). Note, however, that for small DNA strands (up to several kilo bases) and high salt conditions the persistence length can be significantly smaller (≈30–35 *nm*), (Kam et al., 1981; Manning, 1981; Post, 1983; Savelyev, 2012; Brunet et al., 2015; Rieger and Virnau, 2018) and also depends on the specific ions in the solvent (Brunet et al., 2015) (the influence of which we neglect as well). Nevertheless, for larger chains (such as those simulated in our paper) persistence length is expected to increase again and might actually be closer to 50 *nm*. In high salt conditions knotting probabilities also depend little on the actual value of the persistence length as demonstrated in Supplementary Information, which taken together justifies our simplified assumptions.

Experiments (Plesa et al., 2016; Kumar Sharma et al., 2019) displayed in Figure 2A use either KCl (1 and 1.5 M) or LiCl (4 M) as buffer. In our simulations we mainly study DNA strands of lengths 20,678 bp, 48,502 bp and 165,648 bp corresponding to a linearized plasmid, λ phage DNA and phage *T4 GT7* DNA used in Plesa et al. (2016).

For comparison we have also implemented a simple random walk which can be mapped onto DNA by setting the Kuhn length to 100 nm, which takes over the role of d from Eq. 3. Interestingly, this simplistic model for DNA was already discussed in the first simulation paper on polymer knots from 1974 (Vologodskii et al., 1974) and yields, as we will see later, surprisingly reasonable results when compared with recent experiments on long DNA strands (Plesa et al., 2016). Of course, differences in knotting probabilities due to varying ionic conditions are not captured in this approach, but could in principle be included following Rybenkov et al. (1993). All chains were simulated with a pivot Monte Carlo algorithm (Madras and Sokal, 1988): After a pivot center is chosen at random, one arm of the polymer is rotated by a random angle around the pivot point and the move is accepted with the Metropolis criterion.

Knot analysis. Knots are defined only for closed chains and characterised by the minimum number of crossings when projected onto a two-dimensional plane (see Figure 1B) (Adams, 1994). The simplest knot, apart from an unknotted ring which is called the unknot (0), is the trefoil (3_1) with three essential crossings. Similarly, the next knot type to follow is the figure-eight knot (4_1) with four crossings. While there is only one knot with three and one knot with four crossings (as indicated by the index), eventually the number of different knots grows exponentially with the crossing number. In addition to prime knots, multiple knots can also be combined on a ring to form so-called composite knots as indicated in the right-most picture of Figure 1B.

Since we have simulated linear chains a closure to connect the two end points of our chains needs to be defined. For this we first connect the two termini with their centre of mass. Along these lines one can then define a closure which emerges from one end, follows the first line, connects to the second one far away from the polymer and ends at the second end of the chain (Virnau et al., 2006). Once the open chain has been closed the Alexander polynomial can be determined for which a detailed description can be found in Virnau (2010). The size of a knot can be determined by successively removing monomers from the two ends of the polymer (before closure) chain until the knot type changes.

Results

First, we investigate knotting probabilities as a function of DNA length and ionic conditions for unconfined DNA (Figure 2A). For better clarity, we only plot fitted curves according to Deguchi and

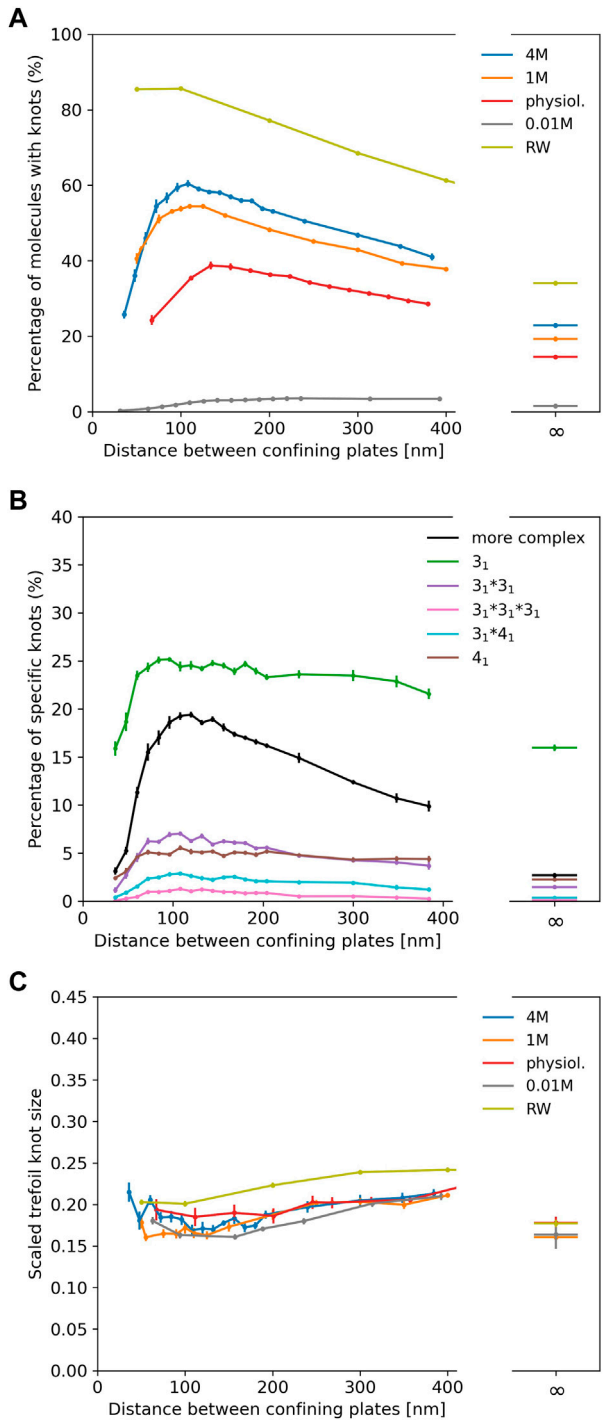

FIGURE 3
(A) Knotting probability of λ phage DNA (48.5 kbp) as a function of plate distance at various ionic conditions in slit-pore confinement. **(B)** Knot spectrum for a salt concentration of 4 M. Complex knots refer to all other knots not listed here excluding the unknot. **(C)** Average sizes of trefoil knots.

Tsurusaki (1997) for our simulated data. Experimental data from recent nanopore experiments (Plesa et al., 2016; Kumar Sharma et al., 2019) on 20,678 bp long linearized plasmids, λ phage (48,502 bp) and *T4 GT7* DNA (165,648 bp) are displayed as data points. We notice that even in the range of 100 kbp, DNA already exhibits substantial knotting which strongly depends on ionic conditions. Knotting probabilities are larger in high salt scenarios and can reach up to 70% for the largest strands. Intriguingly, our coarse-grained simulations also suggest that knotting can almost be avoided completely in a low salt scenario. For the same 166 kbp strand we only observe a knotting probability of 5%, which (if confirmed experimentally) would open up new possibilities for disentangling large DNA strands, e.g., in preparation of nanopore sequencing. The latter may, however, prove challenging experimentally as it becomes difficult to translocate at low ionic concentrations. These large discrepancies are indeed surprising as prior simulations of closed DNA rings with a similar model yielded significantly higher knotting probabilities, particularly for the low salt scenario (Dai et al., 2012b). Overall, agreement between predicted and experimentally determined knotting probabilities in medium to high salt conditions is quite good and differences only amount to a few percent. Surprisingly, comparisons with a simple random walk model still yield reasonable agreement even though occurrences of knots are overestimated systematically. At the length scales considered, the knot spectrum is still dominated by trefoil knots as is depicted for the high salt (4 M) scenario in Figure 2B. However, we already observe the emergence of composite knots as demonstrated before for even larger chains under physiological conditions in Rieger and Virnau (2016).

In Figure 3A we show results for λ phage DNA (48,502 bp) confined between two plates to study the interplay of ionic conditions with confinement. As no experimental data is available, Figure 3A only displays simulation results. The general shape of the curves follows results for shorter chains and high ionic conditions from Micheletti and Orlandini (2012a), Orlandini and Micheletti (2013) and for rings in Dai et al. (2012b): The knotting probability first increases with increasing plate distance, reaches a maximum at around 100–150 nm before falling off and approaching the value obtained for unconfined DNA. Here, we note again that knotting is suppressed substantially in low salt scenarios. For all salt concentrations, the number of knotted conformations in comparison to unconfined DNA is roughly increased by a factor of two at the maximum, and the position of the maximum shifts to lower plate distances with increasing salt concentrations as noted for closed rings in Dai et al. (2012b).

Figure 3B displays the knot spectrum as a function of plate distance for the 4 M high salt scenario. While the amount of complex knots decreases (and unknots thus increase) for distances beyond the maximum, the composition of trefoil, figure-eight and composite variants of the two only varies slightly.

In Figure 3C, we plot the scaled trefoil knot length (which we define as the ratio of the contour length of the trefoil knot to the contour length of the whole chain). For all concentrations and plate distances, a trefoil knot roughly occupies one-fifth of the chain and has a similar size as in the unconfined scenario. For a simple random walk, we roughly obtain the same result.

Discussion

We investigate with numerical simulations the influence of ionic conditions on knotting of free DNA and DNA confined between two

plates with a focus on long, experimentally relevant strands. From a technical point of view we test and confirm a coarse-grained bead-stick model by comparing simulations to recent nanopore experiments on DNA knotting. The model is not only susceptible to the influence of ionic conditions and reproduces the existing experimental knotting probabilities for unconfined DNA, but also resolves the structure of DNA below the persistence length. As such it is well-suited for the numerical description of recent (Plesa et al., 2016; Kumar Sharma et al., 2019) and ongoing DNA experiments in the range of tens to hundreds of kilo base pairs and could be easily adapted for molecular dynamics simulations. Extensions which account for smaller, varying persistence lengths in small strands could be implemented as well to study structural properties of DNA at these scales (Zoli, 2018). At large length scales we observe a strong dependence on solvent conditions: While knotting can be abundant in a high salt scenario in which negative charges on DNA are completely screened, it becomes almost negligible in low salt conditions. Experiments on DNA dynamics (Shusterman et al., 2004) also imply that characteristic time scales involved in these transitions may well be below typical times required, e.g., for nanopore sequencing even though further studies on this issue are certainly warranted. If this drastic change is confirmed experimentally in long strands, an adjustment of ionic conditions could indeed be used as a switch to effectively unknot DNA in scenarios where knots are undesired. Likewise, such experiments could further improve coarse-grained models by eliminating the need to assume effective excluded volume interactions, which could be fitted to knotting probabilities instead (Rieger and Virnau, 2016; Rieger and Virnau, 2018).

Data availability statement

The raw data supporting the conclusions of this article will be made available by the authors, without undue reservation.

Author contributions

SW: Simulation and analysis (lead); software (equal); writing of original draft (equal). RD: Simulation and topological analysis (supporting); software (supporting); writing of original draft (equal). PV: Conceptualization (lead); funding acquisition (lead); methodology (lead); supervision (lead); writing (lead); software (equal).

Acknowledgments

We are grateful to the Deutsche Forschungsgemeinschaft (DFG, German Research Foundation) for funding this research: Project number 233630050-TRR 146 and 464588647-CRC 1551. The authors also acknowledge computing time granted on the supercomputer Mogon offered by the Johannes Gutenberg University Mainz (hpc.uni-mainz.de), which is a member of the AHRP (Alliance for High Performance Computing in Rhineland Palatinate, www.ahrp.info) and the Gauss Alliance e.V. P.V. would also like to acknowledge helpful discussions with Eugene Kim.

Conflict of interest

The authors declare that the research was conducted in the absence of any commercial or financial relationships that could be construed as a potential conflict of interest.

Publisher's note

All claims expressed in this article are solely those of the authors and do not necessarily represent those of their affiliated organizations, or those of the publisher, the editors and the reviewers. Any product that may be evaluated in this article, or claim that may be made by its manufacturer, is not guaranteed or endorsed by the publisher.

Supplementary material

The Supplementary Material for this article can be found online at: https://www.frontiersin.org/articles/10.3389/fchem.2022.1096014/full#supplementary-material

References

Adams, C. C. (1994). *The knot book*. Rhode Island: American Mathematical Soc.

Amin, S., Khorshid, A., Zeng, L., Zimmy, P., and Reisner, W. (2018). A nanofluidic knot factory based on compression of single DNA in nanochannels. *Nat. Commun.* 9, 1506. doi:10.1038/s41467-018-03901-w

Brunet, A., Tardin, C., Salomé, L., Rousseau, P., Destainville, N., and Manghi, M. (2015). Dependence of DNA persistence length on ionic strength of solutions with monovalent and divalent salts: A joint theory–experiment study. *Macromolecules* 48, 3641–3652. doi:10.1021/acs.macromol.5b00735

Dai, L., Jones, J. J., van der Maarel, J. R. C., and Doyle, P. S. (2012a). A systematic study of DNA conformation in slitlike confinement. *Soft Matter* 8, 2972–2982. doi:10.1039/C2SM07322F

Dai, L., Renner, C. B., and Doyle, P. S. (2015). Metastable knots in confined semiflexible chains. *Macromolecules* 48, 2812–2818. doi:10.1021/acs.macromol.5b00280

Dai, L., van der Maarel, J. R. C., and Doyle, P. S. (2012b). Effect of nanoslit confinement on the knotting probability of circular DNA. *ACS Macro Lett.* 1, 732–736. doi:10.1021/mz3001622

Deguchi, T., and Tsurusaki, K. (1997). Universality of random knotting. *Phys. Rev. E* 55, 6245–6248. doi:10.1103/PhysRevE.55.6245

Delbrück, M. (1962). "Knotting problems in biology," in *Mathematical problems in biological sciences*. Editor R. E. Bellman (Rhode Island: American Mathematical Society). vol. 14 of Proc. Symp. Appl. Math, 55.

Di Stefano, M., Tubiana, L., Di Ventra, M., and Micheletti, C. (2014). Driving knots on DNA with ac/dc electric fields: Topological friction and memory effects. *Soft Matter* 10, 6491–6498. doi:10.1039/C4SM00160E

Fisher, M. E. (1964). Magnetism in one-dimensional systems—The Heisenberg model for infinite spin. *Am. J. Phys.* 32, 343–346. doi:10.1119/1.1970340

Frisch, H. L., and Wasserman, E. (1961). Chemical topology 1. *J. Am. Chem. Soc.* 83, 3789–3795. doi:10.1021/ja01479a015

Ganji, M., Shaltiel, I. A., Bisht, S., Kim, E., Kalichava, A., Haering, C. H., et al. (2018). Real-time imaging of DNA loop extrusion by condensin. *Science* 360, 102–105. doi:10.1126/science.aar7831

Hill, T. (1960). *Introduction to statistical thermodynamics*. Boston: Adison-Wesley.

Hill, T. (1956). *Statistical mechanics*. New York, USA: McGraw-Hill.

Jain, A., and Dorfman, K. D. (2017). Simulations of knotting of DNA during genome mapping. *Biomicrofluidics* 11, 024117. doi:10.1063/1.4979605

Jain, M., Koren, S., Miga, K. H., Quick, J., Rand, A. C., Sasani, T., et al. (2018). Nanopore sequencing and assembly of a human genome with ultra-long reads. *Nat. Biotechnol.* 36, 338–345. doi:10.1038/nbt.4060

Jain, M., Olsen, H., Benedict, P., and Akerson, M. (2016). The oxford nanopore minION: Delivery of nanopore sequencing to the genomics community. *Genome Biol.* 17, 239. doi:10.1186/s13059-016-1103-0

Kam, Z., Borochov, N., and Eisenberg, H. (1981). Dependence of laser light scattering of DNA on NaCl concentration. *Biopolymers* 20, 2671–2690. doi:10.1002/bip.1981.360201213

Kratky, O., and Porod, G. (1949). Röntgenuntersuchung gelöster Fadenmoleküle. *Recl. Des. Trav. Chim. Des. Pays-Bas* 68, 1106–1122. doi:10.1002/recl.19490681203

Kumar Sharma, R., Agrawal, I., Dai, L., Doyle, P. S., and Garaj, S. (2019). Complex DNA knots detected with a nanopore sensor. *Nat. Commun.* 10, 4473. doi:10.1038/s41467-019-12358-4

Lieberman-Aiden, E., van Berkum, N. L., Williams, L., Imakaev, M., Ragoczy, T., Telling, A., et al. (2009). Comprehensive mapping of long-range interactions reveals folding principles of the human genome. *Science* 326, 289–293. doi:10.1126/science.1181369

Lua, R., Borovinskiy, A. L., and Grosberg, A. Y. (2004). Fractal and statistical properties of large compact polymers: A computational study. *Polymer* 45, 717–731. Conformational Protein Conformations. doi:10.1016/j.polymer.2003.10.073

Madras, N., and Sokal, A. D. (1988). The pivot algorithm: A highly efficient Monte Carlo method for the self-avoiding walk. *J. Stat. Phys.* 50, 109–186. doi:10.1007/BF01022990

Manning, G. S. (1981). A procedure for extracting persistence lengths from light-scattering data on intermediate molecular weight DNA. *Biopolymers* 20, 1751–1755. doi:10.1002/bip.1981.360200815

Marenduzzo, D., Orlandini, E., Stasiak, A., Sumners, D. W., Tubiana, L., and Micheletti, C. (2009). DNA–DNA interactions in bacteriophage capsids are responsible for the observed DNA knotting. *Proc. Natl. Acad. Sci.* 106, 22269–22274. doi:10.1073/pnas.0907524106

Marenz, M., and Janke, W. (2016). Knots as a topological order parameter for semiflexible polymers. *Phys. Rev. Lett.* 116, 128301. doi:10.1103/PhysRevLett.116.128301

McMillan, W. G., and Mayer, J. E. (1945). The statistical thermodynamics of multicomponent systems. *J. Chem. Phys.* 13, 276–305. doi:10.1063/1.1724036

Micheletti, C., and Orlandini, E. (2012a). Knotting and metric scaling properties of DNA confined in nano-channels: A Monte Carlo study. *Soft Matter* 8, 10959–10968. doi:10.1039/C2SM26401C

Micheletti, C., and Orlandini, E. (2014). Knotting and unknotting dynamics of DNA strands in nanochannels. *ACS Macro Lett.* 3, 876–880. doi:10.1021/mz500402s

Micheletti, C., and Orlandini, E. (2012b). Numerical study of linear and circular model DNA chains confined in a slit: Metric and topological properties. *Macromolecules* 45, 2113–2121. doi:10.1021/ma202503k

Odijk, T. (1977). Polyelectrolytes near the rod limit. *J. Polym. Sci. Polym. Phys. Ed.* 15, 477–483. doi:10.1002/pol.1977.180150307

Orlandini, E., and Micheletti, C. (2013). Knotting of linear DNA in nano-slits and nano-channels: A numerical study. *J. Biol. Phys.* 39, 267–275. doi:10.1007/s10867-013-9305-0

Plesa, C., Verschueren, D., Pud, S., van der Torre, J., Ruitenberg, J. W., Witteveen, M. J., et al. (2016). Direct observation of DNA knots using a solid-state nanopore. *Nat. Nanotechnol.* 11, 1093–1097. doi:10.1038/nnano.2016.153

Post, C. B. (1983). Excluded volume of an intermediate-molecular-weight DNA. a Monte Carlo analysis. *Biopolymers* 22, 1087–1096. doi:10.1002/bip.360220406

Reith, D., Cifra, P., Stasiak, A., and Virnau, P. (2012). Effective stiffening of DNA due to nematic ordering causes DNA molecules packed in phage capsids to preferentially form torus knots. *Nucleic acids Res.* 40, 5129–5137. doi:10.1093/nar/gks157

Renner, C. B., and Doyle, P. S. (2014). Untying knotted DNA with elongational flows. *ACS Macro Lett.* 3, 963–967. doi:10.1021/mz500464p

Rieger, F. C., and Virnau, P. (2016). A Monte Carlo study of knots in long double-stranded DNA chains. *Plos Comput. Biol.* 12, e1005029. doi:10.1371/journal.pcbi.1005029

Rieger, F. C., and Virnau, P. (2018). Coarse-grained models of double-stranded DNA based on experimentally determined knotting probabilities. *React. Funct. Polym.* 131, 243–250. doi:10.1016/j.reactfunctpolym.2018.08.002

Rothörl, J., Wettermann, S., Virnau, P., and Bhattacharya, A. (2022). Knot formation of dsDNA pushed inside a nanochannel. *Sci. Rep.* 12, 5342. doi:10.1038/s41598-022-09242-5

Rybenkov, V. V., Cozzarelli, N. R., and Vologodskii, A. V. (1993). Probability of DNA knotting and the effective diameter of the DNA double helix. *Proc. Natl. Acad. Sci. U. S. A.* 90, 5307–5311. doi:10.1073/pnas.90.11.5307

Savelyev, A. (2012). Do monovalent mobile ions affect DNA's flexibility at high salt content? *Phys. Chem. Chem. Phys.* 14, 2250–2254. doi:10.1039/C2CP23499H

Shaw, S., and Wang, J. (1994). Knotting of a DNA chain during ring closure. *Science* 260, 533–536. doi:10.1126/science.8475384

Shusterman, R., Alon, S., Gavrinyov, T., and Krichevsky, O. (2004). Monomer dynamics in double- and single-stranded DNA polymers. *Phys. Rev. Lett.* 92, 048303. doi:10.1103/PhysRevLett.92.048303

Siebert, J. T., Kivel, A. N., Atkinson, L. P., Stevens, T. J., Laue, E. D., and Virnau, P. (2017). Are there knots in chromosomes? *Polymers* 9, 317. doi:10.3390/polym9080317

Skolnick, J., and Fixman, M. (1977). Electrostatic persistence length of a wormlike polyelectrolyte. *Macromolecules* 10, 944–948. doi:10.1021/ma60059a011

Stevens, T. J., Lando, D., Basu, S., Atkinson, L. P., Cao, Y., Lee, S. F., et al. (2017). 3D structures of individual mammalian genomes studied by single-cell Hi-C. *Nature* 544, 59–64. doi:10.1038/nature21429

Stigter, D. (1977). Interactions of highly charged colloidal cylinders with applications to double-stranded DNA. *Biopolymers* 16, 1435–1448. doi:10.1002/bip.1977.360160705

Suma, A., Di Stefano, M., and Micheletti, C. (2018). Electric-field-driven trapping of polyelectrolytes in needle-like backfolded states. *Macromolecules* 51, 4462–4470. doi:10.1021/acs.macromol.8b00019

Suma, A., and Micheletti, C. (2017). Pore translocation of knotted DNA rings. *Proc. Natl. Acad. Sci.* 114, E2991–E2997. doi:10.1073/pnas.1701321114

Tang, J., Du, N., and Doyle, P. S. (2011). Compression and self-entanglement of single DNA molecules under uniform electric field. *Proc. Natl. Acad. Sci.* 108, 16153–16158. doi:10.1073/pnas.1105547108

Trefz, B., Siebert, J., and Virnau, P. (2014). How molecular knots can pass through each other. *Proc. Natl. Acad. Sci.* 111, 7948–7951. doi:10.1073/pnas.1319376111

Virnau, P. (2010). Detection and visualization of physical knots in macromolecules. *Phys. Procedia* 6, 117–125. doi:10.1016/j.phpro.2010.09.036

Virnau, P., Kantor, Y., and Kardar, M. (2005). Knots in globule and coil phases of a model polyethylene. *J. Am. Chem. Soc.* 127, 15102–15106. doi:10.1021/ja052438a

Virnau, P., Mirny, L. A., and Kardar, M. (2006). Intricate knots in proteins: Function and evolution. *PLoS Comput. Biol.* 2, e122. doi:10.1371/journal.pcbi.0020122

Vologodskii, A., Lukashin, A., and Frank-Kamenetskiĭ, M. D. (1974). Topological interaction between polymer chains. *Sov. Phys.-JETP* 40, 932–936.

Zoli, M. (2018). Short DNA persistence length in a mesoscopic helical model. *Europhys. Lett.* 123, 68003. doi:10.1209/0295-5075/123/68003